

# Characterization of Noise in CMOS Ring Oscillators at Cryogenic Temperatures

Prashansa Mukim, Pragma R. Shrestha, Advait Madhavan, Nitin Prasad *Member, IEEE*, Jason Campbell, Forrest D. Brewer *Senior Member, IEEE*, Mark D. Stiles *Fellow, IEEE*, and Jabez J. McClelland

**Abstract**—Allan deviation provides a means to characterize the time-dependence of noise in oscillators and potentially identify the source characteristics. Measurements on a 130 nm, 7-stage ring oscillator show that the Allan deviation declines from 300 K to 150 K as expected, but surprisingly increases from 150 K to 11 K. At low temperatures, the measured Allan deviation can be well fit using a few random telegraph noise (RTN) sources over the range of a few kilohertz to a few gigahertz. Further, the RTN characteristics evolve to reveal an enhanced role in low-frequency noise at lower temperatures.

**Index Terms**—Allan deviation, CMOS ring oscillator, noise, random telegraph noise, temperature, traps

## I. INTRODUCTION

Electronic circuits utilized in space applications, high-energy physics experiments, and high-performance and quantum computing often operate at cryogenic temperatures [1]–[3]. For quantum computing, there is a growing interest in developing control and readout circuitry that operates reliably at temperatures as low as 4 K [4], [5] so as to place it physically close to the qubits and reduce the impact of parasitics in the measurement pathway. Complementary metal-oxide-semiconductor (CMOS) technology is one of the most viable ways to fulfil this need for reliable low-temperature electronics due to its low cost, scalability, and ease of fabrication.

Characterization of the performance of various CMOS technologies at cryogenic temperatures [6]–[9] has been mostly limited to measurements and modeling of dc transistor characteristics. There is relatively limited work devoted to understanding how changes in device characteristics with temperature affect the performance of circuits [10]. Ring oscillators

Submitted on 06/xx/2023. P.M. and N.P. acknowledge support under the Cooperative Research Agreement between the University of Maryland College Park (UMCP) and the National Institute of Standards and Technology (NIST), Physical Measurement Laboratory, award 70NANB18H165, through UMCP. A.M. acknowledges support under assistance award 70NANB21H091 from the U.S. Department of Commerce, NIST.

P.M. and N.P. were with the UMCP, MD 20742 USA and Associates at NIST, Gaithersburg, MD 20899 USA. P.M. is now with Brookhaven National Laboratory, Upton, NY 11973 (e-mail: pmukim@bnl.gov). N.P. is now with IBM Research, Albany, NY (e-mail: nitinprasad@ibm.com).

A.M. is with the UMCP, MD 20742 USA and an Associate at NIST, Gaithersburg, MD 20899 USA (e-mail: advait.madhavan@nist.gov).

P.R.S., J.C., M.D.S. and J.J.M. are with NIST, Gaithersburg, MD 20899 USA (e-mail: {pragya.shrestha, jason.campbell, mark.stiles, jabez.mcclelland}@nist.gov).

F.D.B. is with the University of California, Santa Barbara, CA 93106 USA (email:forrest@ece.ucsb.edu)

are basic building blocks of many digital and mixed-signal integrated circuits, particularly in applications involving timing generation or measurement [11]–[13]. Measuring their properties provides a valuable platform in understanding how low temperatures affect device transient and noise properties.

Measurement of the temperature dependence of timing jitter or phase noise in the oscillator is as important for any practical application as characterization of parameters like frequency and power consumption [14]–[17], but direct measurements of phase noise do not reveal subtle details of the underlying fundamental noise sources. Here, we report measurements of the Allan deviation [18]–[20], a time-domain stability metric, of a 7-stage CMOS ring oscillator as a function of temperature. By creating fits for the Allan deviation with white,  $1/f$  and random telegraph noise (RTN) sources, we are able to trace how the noise signatures for devices in this process evolve with temperature. Our results highlight the use of Allan deviation measurements of ring oscillators to characterize the noise properties of devices from a few kilohertz to a few gigahertz. Noise characterization across a wide range of frequencies provides information about both long-term absolute jitter accumulation and short-term dynamics such as cycle-to-cycle jitter in oscillators [21].

## II. EXPERIMENTAL SETUP

The 7-stage ring oscillator circuit was fabricated in a 130 nm bulk CMOS technology operated at voltages up to 1.5 V. It consists of seven two-input NAND gates [22] with both n-type and p-type transistors sized with a length of 120 nm and width of 8  $\mu\text{m}$ . We wire-bonded the chip to an FR4 [23] printed circuit board with a temperature sensor mounted close to the chip. NP0 [24] ceramic capacitors that perform well down to 4 K, decoupled the on-board power supply. A closed-cycle refrigerator in a cryo-chamber cooled the board.

The timing noise in the oscillator output was characterized with modified Allan deviation [18]–[20], which measures the fractional frequency fluctuations in oscillators as a function of the measurement time interval. Unlike cycle-jitter or cycle-to-cycle jitter [21], Allan deviation captures the dynamics of noise accumulation. We sampled the oscillator output at 50 GHz with a mixed-signal oscilloscope with 130 fs sampling jitter and collected 10 ms time traces. The times at which the output waveform rising edge is at 50 % of its maximum value were used for computing the modified Allan deviation.

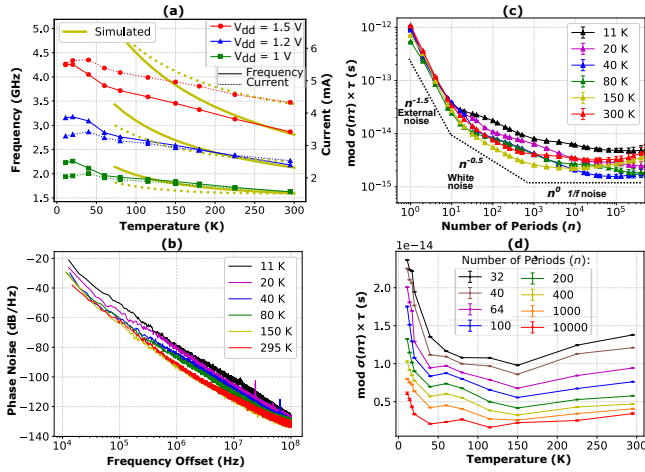


Fig. 1. Measured (a) frequency and current consumption vs. temperature, (b) phase noise power relative to carrier power measured by an oscilloscope (c) modified Allan deviation ( $\text{mod } \sigma(n\tau)$ )  $\times$  oscillator period ( $\tau$ ) vs. number of periods ( $n$ ) at different temperatures (d)  $\text{mod } \sigma(n\tau) \times \tau$  vs. temperature at different values of  $n$ ; error bars in (c) and (d) represent 95 % confidence and are determined from  $\chi^2$  statistics [18].

### III. RESULTS AND DISCUSSION

We interpret the oscillator frequency and current consumption as a function of temperature, as shown in Fig. 1(a), in terms of the typical increase in both carrier mobility ( $\mu$ ) and transistor threshold voltage ( $V_t$ ) [4], [6]–[8]. Then, the current increase from 300 K to 40 K would be due to the increased  $\mu$ , and the drop in current from 40 K to 20 K would be due to the increase in  $V_t$  outweighing the effect of a larger  $\mu$ . The oscillation frequency is inversely proportional to the output capacitance of each gate and proportional to the charging and discharging current. When cooling from 300 K to 40 K, the oscillation frequency increases due to the current increase but from 40 K to 20 K, the current *decreases* and the oscillation frequency *increases*. While gate capacitances are largely temperature independent [25], we speculate that the drain/source depletion capacitance may decrease due to incomplete ionization and higher depletion widths below 40 K, leading to an increase in frequency. The relative frequency increase at 11 K changes from 48 % at  $V_{dd} = 1.5$  V to 44 % at  $V_{dd} = 1.2$  V and 37 % at  $V_{dd} = 1$  V. We presume the increased  $V_t$  affects the current more at lower values of  $V_{dd}$ . Fig. 1(a) also includes SPICE simulation results using room temperature transistor models whose DC operating point simulations show both higher  $\mu$  and higher  $V_t$  at lower temperatures. The simulated trends start diverging from the measured trends as the temperature is lowered, but the same behavior of current increase, frequency increase, and larger frequency increase for higher values of  $V_{dd}$  is seen in both.

Noise sources with power-law characteristics in frequency can be identified by the slope of the Allan deviation on a log-log scale. For the smallest number of periods, the Allan deviation is frequently dominated by high-frequency white noise sources external to the oscillator circuit, with a slope of  $-1.5$ , followed by contributions from noise internal to the oscillator with slopes of  $-0.5$  from white noise and  $0$  from  $1/f$

noise [18]–[20]. The Allan deviation from multiple sources is the square root of the sum of the Allan variances. Fig. 1(c) and Fig. 1(d) show the measured modified Allan deviation. Although the oscillator noise depends on  $V_{dd}$ , we focus on characterizing the temperature dependence of noise at a single value of  $V_{dd} = 1.2$  V lying in the middle of the oscillator’s operating range. To compare results at different temperatures, we scale the modified Allan deviation by the temperature-dependent oscillator period and plot it as a function of the number of periods. We *expect* the deviations to decrease at lower temperatures for several reasons. First, the thermal noise in the drain current should decrease as the temperature is lowered [26]. Although the thermal noise is proportional to the small-signal transconductance, which increases as the temperature is lowered, it only does so by 2 to 3 times for a factor of 70 reduction in temperature [7], [8], [27]. Second, the impulse sensitivity function [28] decreases with faster rise and fall times, which can be inferred from the higher frequencies at lower temperatures in Fig. 1(a), leading to lower conversion of noise to timing jitter. Third,  $1/f$  noise is predicted to decrease by McWhorter’s model [29], [30]. However, at 80 K, the Allan deviation is *higher* than at 300 K for 100 to 1000 periods and becomes higher at all time scales as the temperature is lowered to 11 K. Although contrary to theoretical predictions, this increase is consistent with measurements on individual devices [27], [31] and fabricated CMOS *LC* oscillators [4] that show  $1/f$  noise increases below  $\approx 150$  K. The phase noise measurements in Fig. 1(b) show the same trend: phase noise at 11 K is  $\approx 10$  dB *higher* than that at 300 K. In addition to the increase in the magnitude of the Allan deviation measurements, there are also intermediary slopes that are not characteristic of white or  $1/f$  noise.

To understand the noise increase seen in our measurements, we first fit the measured Allan deviation using a sum of lines of slopes  $-1.5$ ,  $-0.5$ , and  $0$  for frequency fluctuations due to external, white, and  $1/f$  noise respectively. The fitting parameters were the magnitudes of these three noise sources, and we obtained fits by minimizing the sum of relative least-squares errors. These noise sources fit the measured data well at 300 K and 150 K, see Fig. 2(a) and Fig. 2(b). At 80 K (Fig. 2(c)), they give a poor fit, indicating that the noise in the circuit at 80 K is not purely white and  $1/f$ . We attribute the poor fit to the Allan deviation to random telegraph noise (RTN), which originates from the switching activity of traps and has a Lorentzian profile in the frequency domain [32]–[35]. Capture and emission of electrons by a trap results in two-state current fluctuations that linearly map to timing deviations [28]. The autocorrelation function for an RTN signal with the characteristic rate  $r$  is  $e^{-rt}$  [32]. By using this expression for the autocorrelation of a RTN signal, the contribution of an RTN source to the Allan variance is:

$$\frac{A^2}{\tau^2} \frac{4}{(rt)^2} (2rt + 4e^{-rt} - e^{-2rt} - 3), \quad (1)$$

with  $t$  the measurement time,  $A$  the RTN jitter magnitude, and  $\tau$  the oscillator period. In the limit  $rt \ll 1$ ,  $\sigma^2(t) \propto rt$ ; when  $rt \gg 1$ ,  $\sigma^2(t) \propto 1/(rt)$  giving the expected dependence of the Allan deviation as  $t^{1/2}$  and  $t^{-1/2}$  where the Lorentzian

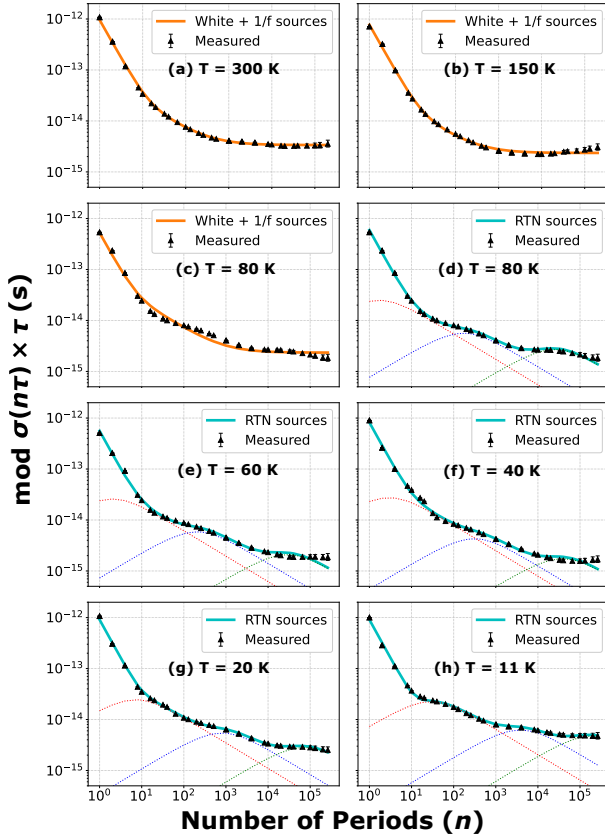


Fig. 2. Fitting measured  $\text{mod } \sigma(n\tau) \times \tau$  using white and flicker noise sources in (a), (b) and (c), RTN sources in (d), (e), (f), (g) and (h). Dotted lines in (d), (e), (f), (g) and (h) show the individual contribution of each RTN source.

shows a  $1/f^2$  roll-off and is flat, respectively.

At and below 80 K, we fit the Allan deviation with a superposition of high-frequency external noise and three RTN sources as in Eq. 1. We model the activity of traps as thermally activated and governed by  $r = r_0 \exp[-\Delta/kT]$ , with  $r_0$  the trap characteristic escape rate,  $\Delta$  the trap activation energy,  $k$  Boltzmann's constant, and  $T$  the temperature. The fitting parameters are temperature-independent values of  $\Delta$  and  $r_0$  for each of the three RTN sources and independent magnitudes for the three sources at each temperature. Fig. 2(d) shows the fit at 80 K obtained with RTN sources, which matches the measured data better than the fit obtained with white and  $1/f$  noise sources. Fits at temperatures below 80 K shown in Fig. 2(e)-(h) also match the measured data closely. Three RTN sources were chosen for these fits as three was the minimum number that led to good fits.

Fig. 3(a) and Fig. 3(b) show the evolution of the frequency and magnitude of the three RTN sources with temperature. Fig. 3(c) shows that below 40 K, the RTN fit error is significantly lower than the fit error with white and  $1/f$  noise. The higher RTN fit error at 40 K and 60 K is primarily due to the slowest trap (trap 3) being less dominant at these temperatures, as can also be seen from the fits in Fig. 2(e) and Fig. 2(f). We expect that there are contributions at all temperatures from white and  $1/f$  sources in addition to the RTN sources, but that different contributions dominate at different temperatures.

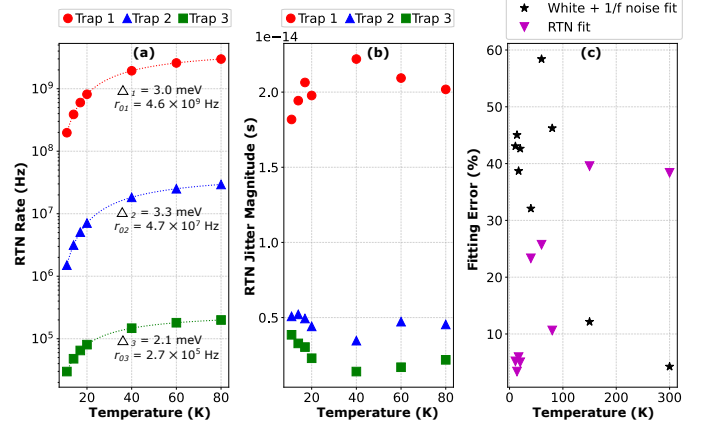


Fig. 3. Evolution of (a) trap frequency, (b) trap noise magnitude and (c) total fitting error vs. temperature.

While a more complicated noise model would result in smaller fitting errors at all temperatures, there is insufficient statistical support for a more complex model in our data. However, the general methodology of fitting measured Allan deviation of ring oscillators to a combination of noise sources enables identification of dominant noise sources at different temperatures.

Our results indicate that for this technology,  $\approx 80$  K is the temperature much below which the observable noise is dominated by the switching activity of ensembles of a few distinct types of traps that emerge from the underlying device defects and much above which is dominated by white and  $1/f$  noise. As the temperature goes down, the rate  $r$  for each of the traps decreases, shifting the peak in the Allan deviation to higher number of periods. The barrier heights ( $\Delta$  values) in Fig. 3(a) found in our fits are consistent with the explanation offered for the increase in measured device  $1/f$  noise due to band-tail states that act as traps at low temperatures [4], [27], [31]. At high temperatures, the band edge traps contribute high-frequency jitter that is obscured by the external noise. As the temperature decreases, the time scales at which the traps contribute decrease and come out from under the high frequency tail, increasing the noise magnitude and changing its profile to RTN in the region otherwise dominated by white and  $1/f$  noise. We attribute the non-trivial temperature dependence seen in Fig. 1(d), especially around 40 - 60 K to (i) dependence of the RTN jitter magnitude ( $A$  in Eq. 1) on the current in Fig. 1(a) (higher current values lead to faster rise/fall times and smaller jitter), and (ii) the period dependence of shifted RTN peaks as traps evolve with temperature.

#### IV. CONCLUSION

Allan deviation measurements probe the noise signatures of a group of devices at cryogenic temperatures from a few kilohertz to a few gigahertz. Such measurements on a 7-stage CMOS ring oscillator show non-monotonic temperature scaling, with a reduction in noise from 300 K to 150 K and a subsequent increase in noise from 150 K to 11 K. This trend is consistent with previously reported individual device measurements that have attributed the increase in noise below 150 K to uncovering of band-tail trap states.



## REFERENCES

- [1] W. Kuhn, N. E. Lay, E. Grigorian, D. Nobbe, I. Kuperman, J. Jeon, K. Wong, Y. Tugunaw, and X. He, "A microtransceiver for UHF proximity links including mars surface-to-orbit applications," *Proceedings of the IEEE*, vol. 95, no. 10, pp. 2019–2044, 2007-10. doi: [10.1109/JPROC.2007.905092](https://doi.org/10.1109/JPROC.2007.905092).
- [2] D. Braga, S. Li, and F. Fahim, "Cryogenic electronics development for high-energy physics: An overview of design considerations, benefits, and unique challenges," *IEEE Solid-State Circuits Magazine*, vol. 13, no. 2, pp. 36–45, 2021. doi: [10.1109/MSSC.2021.3072804](https://doi.org/10.1109/MSSC.2021.3072804).
- [3] B. Prabowo, G. Zheng, M. Mehrpoo, B. Patra, P. Harvey-Collard, J. Dijkema, A. Sammak, G. Scappucci, E. Charbon, F. Sebastiano, L. M. K. Vandersypen, and M. Babaie, "A 6-to-8 GHz 0.17mW/qubit cryo-CMOS receiver for multiple spin qubit readout in 40nm CMOS technology," in *2021 IEEE International Solid-State Circuits Conference (ISSCC)*, pp. 212–214, IEEE, 2021-02-13. doi: [10.1109/ISSCC42613.2021.9365848](https://doi.org/10.1109/ISSCC42613.2021.9365848).
- [4] B. Patra, R. M. Incandela, J. P. G. van Dijk, H. A. R. Homulle, L. Song, M. Shahmohammadi, R. B. Staszewski, A. Vladimirescu, M. Babaie, F. Sebastiano, and E. Charbon, "Cryo-CMOS circuits and systems for quantum computing applications," *IEEE Journal of Solid-State Circuits*, vol. 53, no. 1, pp. 309–321, 2018-01. doi: [10.1109/JSSC.2017.2737549](https://doi.org/10.1109/JSSC.2017.2737549).
- [5] S. J. Pauka, K. Das, R. Kalra, A. Moini, Y. Yang, M. Trainer, A. Bousquet, C. Cantaloube, N. Dick, G. C. Gardner, M. J. Manfra, and D. J. Reilly, "A cryogenic CMOS chip for generating control signals for multiple qubits," *Nature Electronics*, vol. 4, no. 1, pp. 64–70, 2021-01-25. doi: [10.1038/s41928-020-00528-y](https://doi.org/10.1038/s41928-020-00528-y).
- [6] R. M. Incandela, L. Song, H. Homulle, E. Charbon, A. Vladimirescu, and F. Sebastiano, "Characterization and compact modeling of nanometer CMOS transistors at deep-cryogenic temperatures," *IEEE Journal of the Electron Devices Society*, vol. 6, pp. 996–1006, 2018. doi: [10.1109/JEDS.2018.2821763](https://doi.org/10.1109/JEDS.2018.2821763).
- [7] A. Beckers, F. Jazaeri, A. Ruffino, C. Bruschini, A. Baschiroto, and C. Enz, "Cryogenic characterization of 28 nm bulk CMOS technology for quantum computing," in *2017 47th European Solid-State Device Research Conference (ESSDERC)*, pp. 62–65, IEEE, 2017-09. doi: [10.1109/ESSDERC.2017.8066592](https://doi.org/10.1109/ESSDERC.2017.8066592).
- [8] A. Beckers, F. Jazaeri, H. Bohuslavskiy, L. Hutin, S. De Franceschi, and C. Enz, "Design-oriented modeling of 28 nm FDSOI CMOS technology down to 4.2 k for quantum computing," in *2018 Joint International EUROSOCI Workshop and International Conference on Ultimate Integration on Silicon (EUROSOCI-ULIS)*, pp. 1–4, IEEE, 2018-03. doi: [10.1109/ULIS.2018.8354742](https://doi.org/10.1109/ULIS.2018.8354742).
- [9] S.-H. Hong, G.-B. Choi, R.-H. Baek, H.-S. Kang, S.-W. Jung, and Y.-H. Jeong, "Low-temperature performance of nanoscale MOSFET for deep-space RF applications," *IEEE Electron Device Letters*, vol. 29, no. 7, pp. 775–777, 2008-07. doi: [10.1109/LED.2008.2000614](https://doi.org/10.1109/LED.2008.2000614).
- [10] D. Prasad, M. Vangala, M. Bhargava, A. Beckers, A. Grill, D. Tierno, K. Nathella, T. Achuthan, D. Pietromonaco, J. Myers, M. Walker, B. Parvais, and B. Cline, "Cryo-computing for infrastructure applications: A technology-to-microarchitecture co-optimization study," in *2022 International Electron Devices Meeting (IEDM)*, pp. 23–5, IEEE, 2022. doi: [10.1109/IEDM45625.2022.10019436](https://doi.org/10.1109/IEDM45625.2022.10019436).
- [11] N. Kurd, J. Barkarullah, R. Dizon, T. Fletcher, and P. Madland, "A multigigahertz clocking scheme for the pentium(R) 4 microprocessor," *IEEE Journal of Solid-State Circuits*, vol. 36, no. 11, pp. 1647–1653, 2001-11. doi: [10.1109/4.962284](https://doi.org/10.1109/4.962284).
- [12] Min Park and M. H. Perrott, "A VCO-based analog-to-digital converter with second-order sigma-delta noise shaping," in *2009 IEEE International Symposium on Circuits and Systems*, pp. 3130–3133, IEEE, 2009-05. doi: [10.1109/ISCAS.2009.5118466](https://doi.org/10.1109/ISCAS.2009.5118466).
- [13] J. Yu, F. F. Dai, and R. C. Jaeger, "A 12-bit vernier ring time-to-digital converter in 0.13  $\mu\text{m}$  CMOS technology," *IEEE Journal of Solid-State Circuits*, vol. 45, no. 4, pp. 830–842, 2010-04. doi: [10.1109/JSSC.2010.2040306](https://doi.org/10.1109/JSSC.2010.2040306).
- [14] J. Burr, "Cryogenic ultra low power CMOS," in *1995 IEEE Symposium on Low Power Electronics. Digest of Technical Papers*, pp. 82–83, IEEE, 1995. doi: [10.1109/LPE.1995.482473](https://doi.org/10.1109/LPE.1995.482473).
- [15] H. Bohuslavskiy, S. Barraud, V. Barral, M. Casse, L. Le Guevel, L. Hutin, B. Bertrand, A. Crippa, X. Jehl, G. Pillonnet, A. G. M. Jansen, F. Arnaud, P. Galy, R. Maurand, S. De Franceschi, M. Sanquer, and M. Vinet, "Cryogenic characterization of 28-nm FD-SOI ring oscillators with energy efficiency optimization," *IEEE Transactions on Electron Devices*, vol. 65, no. 9, pp. 3682–3688, 2018-09. doi: [10.1109/TED.2018.2859636](https://doi.org/10.1109/TED.2018.2859636).
- [16] I. V. Vernik, T. A. Ohki, M. B. Ketchen, and M. Bhushan, "Performance characterization of PD-SOI ring oscillators at cryogenic temperatures," in *2010 IEEE International SOI Conference (SOI)*, pp. 1–2, IEEE, 2010-10. doi: [10.1109/SOI.2010.5641394](https://doi.org/10.1109/SOI.2010.5641394).
- [17] R. Saligram, W. Chakraborty, N. Cao, Y. Cao, S. Datta, and A. Raychowdhury, "Power performance analysis of digital standard cells for 28 nm bulk CMOS at cryogenic temperature using BSIM models," *IEEE Journal on Exploratory Solid-State Computational Devices and Circuits*, vol. 7, no. 2, pp. 193–200, 2021-12. doi: [10.1109/JX-CDC.2021.3131100](https://doi.org/10.1109/JX-CDC.2021.3131100).
- [18] W. Riley and D. Howe, "Handbook of frequency stability analysis," July 2008.
- [19] D. Allan, "Statistics of atomic frequency standards," *Proceedings of the IEEE*, vol. 54, no. 2, pp. 221–230, 1966. doi: [10.1109/PROC.1966.4634](https://doi.org/10.1109/PROC.1966.4634).
- [20] D. Allan and J. Barnes, "A modified 'Allan Variance' with increased oscillator characterization ability," in *Thirty Fifth Annual Frequency Control Symposium*, pp. 470–475, IEEE, 1981. doi: [10.1109/FREQ.1981.200514](https://doi.org/10.1109/FREQ.1981.200514).
- [21] F. Herzel and B. Razavi, "A study of oscillator jitter due to supply and substrate noise," *IEEE Transactions on Circuits and Systems II: Analog and Digital Signal Processing*, vol. 46, no. 1, pp. 56–62, 1999-01. doi: [10.1109/82.749085](https://doi.org/10.1109/82.749085).
- [22] T. Hoque, M. Mustapa, F. Amsaad, and M. Niamat, "Assessment of NAND based ring oscillator for hardware trojan detection," in *2015 IEEE 58th International Midwest Symposium on Circuits and Systems (MWSCAS)*, pp. 1–4, IEEE, 2015-08. doi: [10.1109/MWSCAS.2015.7282110](https://doi.org/10.1109/MWSCAS.2015.7282110).
- [23] FR4 describes a group of fiberglass epoxy resin materials that conform to National Electrical Manufacturers Association standard LI 1-1998.
- [24] F. Teyssandier and D. Prèle, "Commercially Available Capacitors at Cryogenic Temperatures," in *Ninth International Workshop on Low Temperature Electronics - WOLTE9*, (Guaraju, Brazil), June 2010.
- [25] R. Asanovski, A. Grill, J. Franco, P. Palestri, A. Beckers, B. Kaczer, and L. Selmi, "New insights on the excess 1/f noise at cryogenic temperatures in 28 nm CMOS and ge MOSFETs for quantum computing applications," in *2022 International Electron Devices Meeting (IEDM)*, pp. 30.5.1–30.5.4, IEEE, 2022-12-03. doi: [10.1109/IEDM45625.2022.10019388](https://doi.org/10.1109/IEDM45625.2022.10019388).
- [26] S. M. Sze and K. K. Ng, *Physics of semiconductor devices*. Wiley-Interscience, 3rd ed., 2007.
- [27] R. Asanovski, A. Grill, J. Franco, P. Palestri, A. Beckers, B. Kaczer, and L. Selmi, "Understanding the excess 1/f noise in MOSFETs at cryogenic temperatures," *IEEE Transactions on Electron Devices*, pp. 1–7, 2023. doi: [10.1109/TED.2022.3233551](https://doi.org/10.1109/TED.2022.3233551).
- [28] A. Hajimiri, S. Limotyrakis, and T. Lee, "Jitter and phase noise in ring oscillators," *IEEE Journal of Solid-State Circuits*, vol. 34, no. 6, pp. 790–804, 1999-06. doi: [10.1109/4.766813](https://doi.org/10.1109/4.766813).
- [29] E. Burstein, A. L. McWhorter, P. H. Miller, D. T. Stevenson, and P. B. Weisz, *Semiconductor Surface Physics*. University of Pennsylvania Press, 1957.
- [30] S. Christensson, I. Lundström, and C. Svensson, "Low frequency noise in MOS transistors—i theory," *Solid-State Electronics*, vol. 11, no. 9, pp. 797–812, 1968. doi: [10.1016/0038-1101\(68\)90100-7](https://doi.org/10.1016/0038-1101(68)90100-7).
- [31] H. Oka, T. Matsukawa, K. Kato, S. Iizuka, W. Mizubayashi, K. Endo, T. Yasuda, and T. Mori, "Toward long-coherence-time si spin qubit: The origin of low-frequency noise in cryo-CMOS," in *2020 IEEE Symposium on VLSI Technology*, pp. 1–2, IEEE, 2020-06. doi: [10.1109/VLSITechnology18217.2020.9265013](https://doi.org/10.1109/VLSITechnology18217.2020.9265013).
- [32] M. Kirton and M. Uren, *Noise in Solid-state Microstructures: A New Perspective on Individual Defects, Interface States and Low-frequency (1/f) Noise*. Advances in physics, Taylor & Francis, 1989.
- [33] D. Fleetwood, H. Xiong, Z.-Y. Lu, C. Nicklaw, J. Felix, R. Schrimpf, and S. Pantelides, "Unified model of hole trapping, 1/f noise, and thermally stimulated current in MOS devices," *IEEE Transactions on Nuclear Science*, vol. 49, no. 6, pp. 2674–2683, 2002-12. doi: [10.1109/TNS.2002.805407](https://doi.org/10.1109/TNS.2002.805407).
- [34] K. P. Cheung and J. P. Campbell, "Non-tunneling origin of the 1/f noise in SiC MOSFET," in *2018 International Conference on IC Design & Technology (ICICDT)*, pp. 165–168, IEEE, 2018-06. doi: [10.1109/ICICDT.2018.8399782](https://doi.org/10.1109/ICICDT.2018.8399782).
- [35] J. Campbell, J. Qin, K. Cheung, L. Yu, J. Suehle, A. Oates, and K. Sheng, "Random telegraph noise in highly scaled nMOSFETs," in *2009 IEEE International Reliability Physics Symposium*, pp. 382–388, IEEE, 2009. doi: [10.1109/IRPS.2009.5173283](https://doi.org/10.1109/IRPS.2009.5173283).